# Catalytic growth in a shared enzyme pool ensures robust control of centrosome size

**Deb Sankar Banerjee**[1,2] **and Shiladitya Banerjee**[1,✉]

[1]Department of Physics, Carnegie Mellon University, Pittsburgh, PA 15213, USA
[2]James Franck Institute, University of Chicago, Chicago, IL 60637, USA

**Accurate regulation of centrosome size is essential for ensuring error-free cell division, and dysregulation of centrosome size has been linked to various pathologies, including developmental defects and cancer. While a universally accepted model for centrosome size regulation is lacking, prior theoretical and experimental work suggest a centrosome growth model involving autocatalytic assembly of the pericentriolic material. Here we show that the autocatalytic assembly model fails to explain the attainment of equal centrosome sizes, which is crucial for error-free cell division. Incorporating latest experimental findings into the molecular mechanisms governing centrosome assembly, we introduce a new quantitative theory for centrosome growth involving catalytic assembly within a shared pool of enzymes. Our model successfully achieves robust size equality between maturing centrosome pairs, mirroring cooperative growth dynamics observed in experiments. To validate our theoretical predictions, we compare them with available experimental data and demonstrate the broad applicability of the catalytic growth model across different organisms, which exhibit distinct growth dynamics and size scaling characteristics.**

Correspondence: *shiladtb@andrew.cmu.edu*

## Introduction

Centrosomes are membraneless organelles that act as microtubule organizing centers during mitotic spindle formation (1). Prior to cell division, centrosomes grow many folds in size by accumulating various types of proteins including microtubule nucleators, in a process known as centrosome maturation (2). Tight control of centrosome size is functionally important for the cell as aberrations in centrosome growth and size can lead to errors in chromosome segregation (3). This may result in aneuploidy, which is associated with a range of problems, including birth defects, developmental abnormalities, and cancer (4–6). Previous work has suggested that centrosomes grow cooperatively and regulate their size through a coordinated assembly of the pericentriolic material, mediated by complex signaling pathways and regulatory proteins (7–10). Despite the significant progress on uncovering the molecular components regulating centrosome assembly (10), a quantitative model connecting the molecular mechanisms of growth to centrosome size regulation is lacking.

Centrosomes are composed of a porous scaffold-like structure (11, 12) known as the pericentriolic material (PCM), organized around a pair of centrioles at the core (Fig. 1A). An individual cell starts with a single centrosome in the G1 phase, undergoes centriole duplication in the S phase, followed by the formation of two centrosomes in the G2/M phase (Fig. 1A). During centrosome maturation, the two spatially separated centrosomes grow in size by adding material to their PCMs from a cytoplasmic pool of building blocks (7, 13–16), while the centrioles themselves do not grow. Following maturation, the two centrosomes achieve equal sizes (8, 9, 13), which is deemed essential in the establishment of a symmetric bipolar spindle (10). This size equality is vital for for ensuring error-free cellular division, as spindle size is directly proportional to centrosome sizes (17). However, the mechanisms by which centrosomes within a cell achieve equal size remain poorly understood.

A variety of qualitative and quantitative models of centrosome size regulation have emerged in recent years. These include the limiting pool theory (13, 18), liquid-liquid phase separation model for PCM assembly (8), reaction-diffusion models (19, 20), and centriole-driven assembly of PCM (7, 9, 10, 21–23). While there is no universally accepted model for centrosome size regulation, all these models indicate a positive feedback mechanism underlying centrosome assembly. For instance, Zwicker et al. (8) described PCM assembly as an autocatalytic process, assembled from a single limiting component undergoing active phase segregation through centriole-mediated chemical activity. While this model captures sigmoidal growth dynamics observed experimentally and the scaling of centrosome size with cell size, autocatalytic growth of centrosome pairs can induce significant discrepancies in size. Small initial differences in centrosome size could be amplified during the process of autocatalytic growth, as the larger centrosome would incorporate more material, thereby outcompeting the smaller one (24).

Another category of models, based on a large body of recent experimental work (7, 9, 21, 24), suggests that PCM assembly occurs locally around the centriole, driven by a positive feedback loop between the PCM components (9). In a recent study, we employed quantitative modeling to demonstrate that localized assembly around the centriole, accompanied by distributed turnover within the PCM, can ensure centrosome size equality (23). However, this model did not take into account positive feedback between PCM components, and was thus unable to capture the cooperative nature of growth dynamics. Thus, none of the existing quantitative models can account for robustness in centrosome size equality in the presence of positive feedback. Furthermore, intracellular noise and the distinct nature of centrioles within the two centrosomes (old mother centriole and new mother

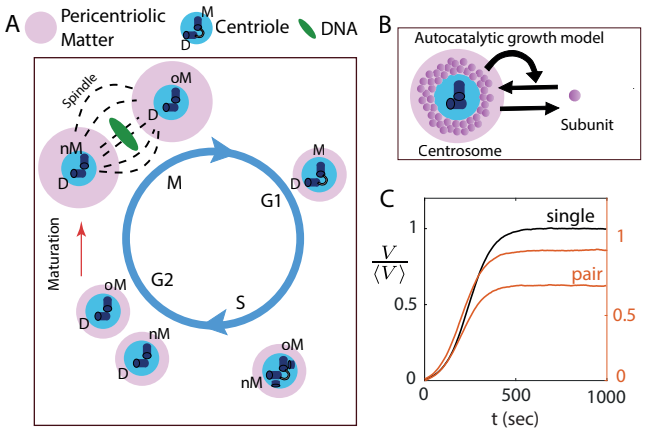


**Fig. 1. Autocatalytic feedback in centrosome growth drives centrosome size inequality.** (A) Schematic showing the dynamics of centrosomes during the cell cycle. In the G1 phase there is a single centrosome with mother (M) and daughter (D) centrioles at the core, surrounded by the pericentriolic material (PCM). The two new centriole pairs with old mother (oM) and new mother (nM) separate into two centrosomes in the G2/M phase after centriole duplication. The spatially separated centrosomes then grow via a process called *centrosome maturation* (red arrow), prior cell division. (B) Schematic of the autocatalytic growth model for centrosomes, where the assembly rate increases with increasing centrosome size. (C) Autocatalytic growth of centrosomes captures the sigmoidal size dynamics for single and a pair of centrosomes, but unable to ensure size equality of a centrosome pair. See Table 1 for a list of parameter values.

centriole, depicted in Fig. 1A) can give rise to fluctuations in centrosome size and introduce initial disparities in size during the maturation process. Consequently, a robust size regulation mechanism is required to achieve centrosome size parity, despite the presence of noise in growth and initial size differences.

Here we present a quantitative theory for size regulation of a centrosome pair via catalytic assembly of the PCM from a cytoplasmic pool of enzymes and molecular components. We first establish that autocatalytic growth of centrosomes in a shared subunit pool results in amplification of initial size differences, leading to significant size inequality after maturation. Then we propose a new model of catalytic growth of centrosomes in a shared pool of building blocks and enzymes. Our theory is based on recent experiments uncovering the interactions of the molecular components of centrosome assembly. We show that this model ensures robust size control of centrosomes while capturing several key features of centrosome growth observed experimentally, including the growth of two stable centrosomes of equal size after maturation (10), sigmoidal growth dynamics (8, 13), tunable scaling of centrosome size with cell size (13), and the ability to robustly create centrosomes of different size from differences in centriole activity (25, 26). We further develop a two-component model of catalytic growth to explicitly show that without the sharing of the enzyme pool, centrosome size regulation is not robust when accounting for the experimentally observed enzyme-mediated positive feedback between the two components (9).

## Results

### Autocatalytic feedback in centrosome growth drives centrosome size inequality.

Previous quantitative modeling of centrosome growth in *C elegans* has suggested that centrosomes are autocatalytic droplets formed via active liquid-liquid phase separation in a limited pool of building blocks (8, 13). Autocatalytic growth arises if centrosome assembly rate increases with centrosome size, creating a size-dependent positive feedback (Fig. 1B). To investigate if autocatalytic growth can ensure size equality of centrosomes, we considered a model of centrosome growth via stochastic assembly and disassembly of its subunits. Though there are multiple essential components involved in PCM assembly (7, 21, 27), we first examined a one-component centrosome model to illustrate the role of autocatalytic growth on size control. The deterministic description for the growth of a centrosome pair is given by

$$\frac{\mathrm{d}n_i}{\mathrm{d}t} = (k_0^+ + k_1^+ n_i(t))\rho(t) - k^- n_i(t)\,, \qquad \textbf{(1)}$$

where $n_i(t)$ is the amount of subunits in $i^{th}$ centrosome ($i = 1,2$), $k_0^+$ and $k_1^+$ are the rate constants for non-cooperative and cooperative assembly, respectively, and $k^-$ is the disassembly rate constant. Eq. (1) can be derived from the phase segregation model for centrosome assembly studied by Zwicker *et al* (8) (see SI section I), with $k_0^+$ and $k_1^+$ representing centriole activity and the strength of autocatalytic interaction, respectively. In Eq. (1), $\rho(t)$ is the cytoplasmic concentration of centrosomal subunits, given by $\rho(t) = (N - n_1(t) - n_2(t))/V_c$ where $V_c$ is cell volume and $N$ is the total amount of subunits in the cell. Centrosome volume is given by $V_i(t) = n_i(t)\delta v$, where $\delta v$ is the effective volume occupied by a single subunit. As shown before (8), this model can capture the essential quantitative features of the growth of a single centrosome (Fig. 1C), including sigmoidal growth curve, temporal control of size and scaling of centrosome size with cell size. However, this model is unable to ensure size equality of two identical centrosomes growing from a shared subunit pool. Stochastic simulation shows significant difference in steady-state size even with a small initial size difference (Fig. 1C).

It is instructive to first compare two opposite limits of the model, $k_0^+ = 0$ (purely autocatalytic growth) and $k_1^+ = 0$ (non-cooperative growth). For $k_0^+ = 0$, Eq. (1) can be interpreted as assembly and disassembly occurring throughout the PCM volume, with the assembly rate scaling with centrosome size. As a result, the centrosome with a larger initial size would end up growing to a larger steady-state size. Stochastic simulations of this model show that the ensemble-averaged absolute difference in centrosome size ($|\delta V| = |V_1 - V_2|$) increases with the initial centrosome size difference ($\delta V_0$), indicating lack of robustness in size regulation (see SI section II and Fig. S1). On the other hand, the limit $k_1^+ = 0$ corresponds to a model where the assembly rate is size-independent, and material turnover is distributed throughout the PCM volume. This model guarantees size equality of a centrosome pair competing for a limiting subunit pool (see SI section II and Fig. S2), even in the presence of large initial size differences (Fig. 2D), with the steady-state size given by $V = k^+ N\delta v/(k^- + 2k^+)$. However, the

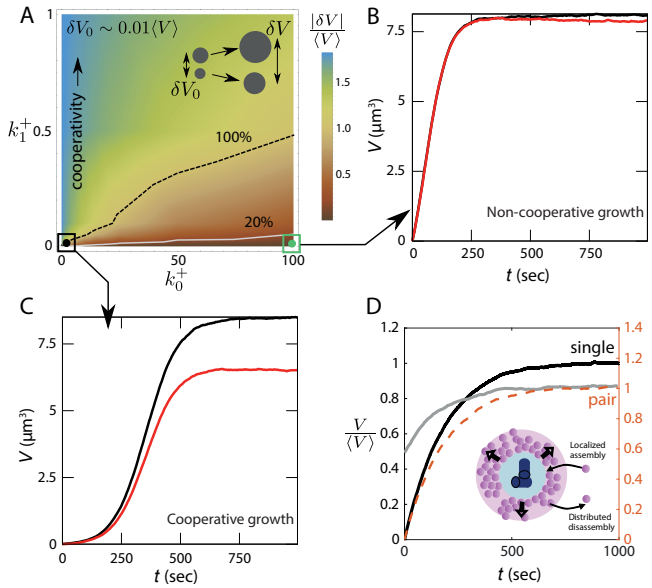


**Fig. 2. Lack of robust size control in autocatalytic growth.** (A) The relative difference in centrosome size, $|\delta V|/\langle V\rangle$, as a function of the growth rate constants $k_0^+$ and $k_1^+$, with an initial size difference of $0.1\ \mu m^3$. The light gray and dashed black lines represent the lines $|\delta V|/\langle V\rangle = 0.2$ and $|\delta V|/\langle V\rangle = 1.0$. (B,C) Size dynamics of a pair centrosomes for (B) weakly cooperative ($k_0^+ = 100$, $k_1^+ = 0.001$) and (C) strongly cooperative ($k_0^+ = 0.1$, $k_1^+ = 0.001$) growth regimes. (D) Dynamics of centrosome size for a single centrosome and a pair of centrosomes simulated using the non-cooperative growth model. Inset: Schematic of centrosome growth via centriole-localized assembly and disassembly distributed throughout the PCM. The $|\delta V|/\langle V\rangle$ values in (A) represent average over $1000$ ensembles. The values of $k_0^+$ and $k_1^+$ are in the units of $\times 600\,\mu M^{-1}\,s^{-1}$. See Table 1 for a list of parameter values.

resulting growth curve is non-sigmoidal, thus fails to capture experimental data in *C. elegans* (8, 13).

To quantify the robustness of size control, we measured the relative difference in steady-state centrosome size, $|\delta V|/\langle V\rangle$, starting with an initial size difference $\delta V_0 \sim 0.01\langle V\rangle$, where $|..|$ denotes the absolute value and $\langle V\rangle$ is the ensemble average of centrosome size at steady-state. The resulting size inequality is controlled by the rate constants $k_0^+$ and $k_1^+$. Our analysis shows that there is a relatively small region of the parameter space where the strength of the autocatalytic feedback is low enough (i.e., $k_0^+ \gg k_1^+$) to ensure small difference in centrosome size (Fig. 2A). However, in this range of parameter values, the growth is essentially non-cooperative and the growth curve is not sigmoidal (Fig. 2B). Larger size inequality is associated with higher values of $k_1^+$, when the growth dynamics is sigmoidal in nature (Fig. 2C). For a detailed study of the lack of robustness in size regulation, please refer to Section I of the Supplementary Information and Figure S3.

## Catalytic growth in a shared enzyme pool ensures centrosome size equality and cooperative growth.

***Model motivation and assumptions.*** Centrosome growth during maturation occurs through the expansion of a scaffold-like structure and subsequent recruitment of PCM proteins on the scaffold. While multiple proteins are involved in the scaffold assembly, Spd-2 and centrosomin (Cnn) are two essential scaffold forming proteins, in the absence of which centrosome growth is almost entirely diminished (7). The kinase Polo interacts with both Spd-2 and Cnn to promote the assembly of a stable scaffold. In particular, Spd-2 recruits Cnn with the help of Polo and Cnn in turn strengthens the Spd-2 scaffold without directly recruiting additional Spd-2 proteins. Without the Polo kinase, the Cnn scaffold fails to grow (9). These findings suggest a model for catalytic assembly of centrosomes based on positive feedback between scaffold-forming proteins and an enzyme. Moreover, Fluorescent Recovery After Photobleaching (FRAP) data reveal that the turnover rate of the enzyme Polo kinase within PCM is much faster ($\sim 1$ min) compared to the Spd-2 and Cnn ($\sim 10$ min) (9, 28). Consequently, owing to the enzyme's pronounced diffusivity, there is a strong likelihood that the active enzyme pool is shared between the two centrosomes.

To ascertain whether a shared catalytic growth model can yield size parity in a pair of centrosomes, we initially formulated a single-component model for PCM growth, catalyzed by an enzyme (Fig. 3A). This model takes into account a shared limiting pool of enzyme and PCM subunits. The assumption of a limiting subunit pool is supported by prior research on *C. elegans*, which displayed centrosome size scaling with centrosome number (13). While the presence of such a limited subunit pool has not been established in other systems, we will subsequently demonstrate that even in cases where centrosome size scaling is not pronounced, the subunit pool can still be finite. Consequently, we implement a model with a limiting pool for both subunits and enzymes. We later relax this assumption by exploring the implications of an infinite enzyme pool.

***Model description.*** In the single-component model for PCM growth, PCM is composed of a single type of subunit that can either take an inactive form ($S_1$), or an enzyme-dependent active form ($S_1^*$), with $S_n$ representing a centrosome with $n$ subunits. The single coarse-grained subunit ($S_1$) represents a composite of the scaffold-forming proteins (e.g., Spd-2 and Cnn in *Drosophila*), and the enzyme ($E$) represents the kinase (e.g., Polo in *Drosophila*). The inactive subunit can slowly bind and unbind from the PCM, while the enzyme-activated form can assemble faster (reactions 1 and 2 in Fig. 3B). The subunit activation is carried out by the active form of the enzyme ($E^*$). Enzyme activation occurs in the PCM, and is thus centrosome size-dependent (reactions 3 and 4 in Fig. 3B). A centrosome with a larger PCM thus produces active enzymes at a faster rate, and an increased amount of activated enzymes enhance centrosome growth. Thus, size-dependent enzyme activation generates a positive feedback in growth, which is shared between the centrosomes as the enzymes activated by each centrosome become part of the shared enzyme pool. This is in contrast to the autocatalytic growth model where the size-dependent positive feedback was exclusive to each centrosome.

A deterministic description for the growth of a single centrosome is given by the coupled dynamics of centrosome size ($S_n$, number of incorporated subunits), the abundance of

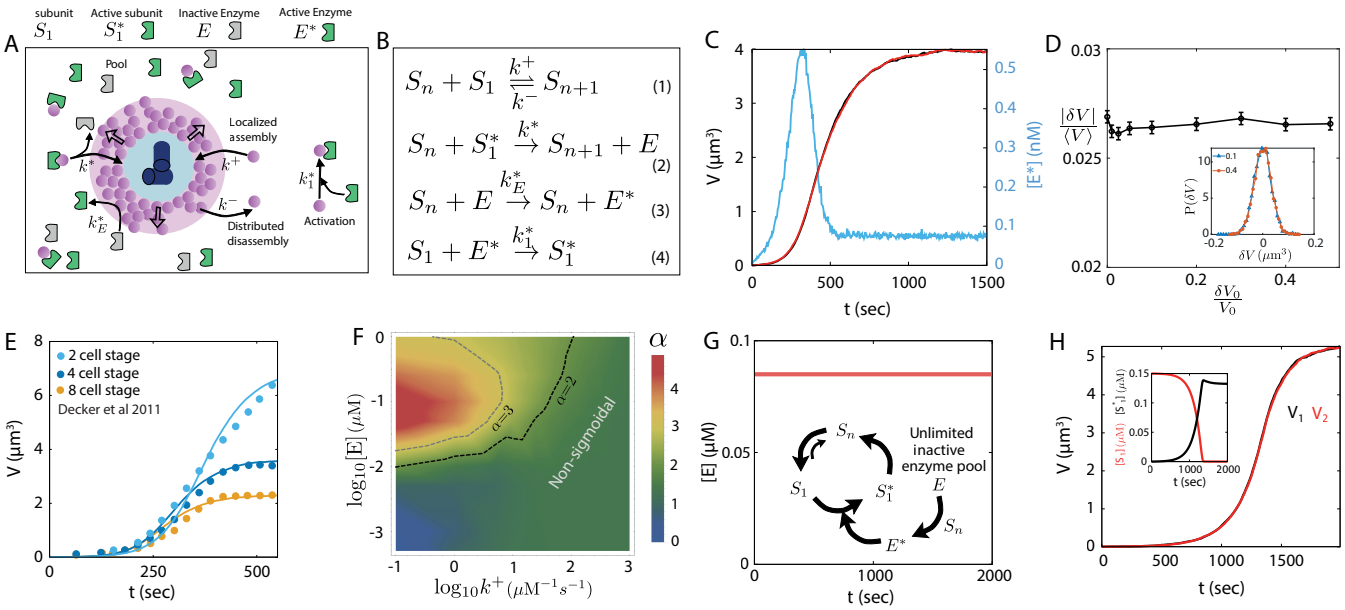


**Fig. 3. Catalytic growth in a shared enzyme pool leads to robust size control of a centrosome pair.** (A) Schematic of centrosome growth via catalytic activity of an enzyme that is activated by PCM proteins at a rate proportional to PCM size. (B) Reactions describing centrosome growth via catalytic activity of enzyme $E$. The centrosome ($S_n$) can activate the enzyme in a state $E^*$, which in turn creates an activated subunit ($S_1^*$) that binds the PCM. (C) Size dynamics of a centrosome pair (blue, red curves) growing via catalytic assembly and the dynamics of the activated enzyme ($[E^*]$) in time (blue curve). (D) The ensemble average of relative absolute size difference $|\delta V|/\langle V \rangle$ is insensitive to change in relative initial size difference $\delta V_0/V_0$. Inset: Probability distribution of $\delta V$ for two different values of initial size difference ($\delta V_0/V_0 = 0.1$ and $\delta V_0/V_0 = 0.4$). (E) Centrosome growth curves obtained from the catalytic growth model (lines) fitted to experimental growth curves (points) measured at different stages of *C. elegans* development. (F) Degree of sigmoidal growth, measured by Hill coefficient $\alpha$, as a function of the growth rate constant $k^+$ and the total enzyme concentration $[E]$. (G) Model of shared catalysis considering a constant concentration of inactive enzyme ($E$) throughout the growth period. Inset: Schematic of the reactions showing the steady state cycle between $S_1$, $S_1^*$ and $S_n$. (H) Centrosome pair growth in the presence of unlimited inactive enzyme pool exhibits size equality as well as cooperative growth dynamics. Inset: Dynamics of $S_1$ and $S_1^*$ concentrations. See Table. 1 for a list of parameter values.

available active subunits ($S_1^*$) and the abundance of activated enzymes ($E^*$):

$$\frac{\mathrm{d}S_n}{\mathrm{d}t} = \frac{k^+}{V_c} N_{av} + \frac{k^*}{V_c} S_1^* - k^- S_n \,, \tag{2}$$

$$\frac{\mathrm{d}S_1^*}{\mathrm{d}t} = \frac{k_1^*}{V_c} N_{av} E^* - \frac{k^*}{V_c} S_1^* \,, \tag{3}$$

$$\frac{\mathrm{d}E^*}{\mathrm{d}t} = \frac{k_E^*}{V_c} S_n N_{av}^E - \frac{k_1^*}{V_c} N_{av} E^* \,, \tag{4}$$

where $k^+$ and $k^*$ are the assembly rates for inactive and active form of the subunit, and $k^-$ is the disassembly rate. The rates for PCM-dependent enzyme activation and enzyme-dependent subunit activation are given by $k_E^*$ and $k_1^*$ (Fig. 3B). The condition for limiting component pool is imposed by substituting $S_1$ and $E$ with the constraints: $S_1 = N - S_n - S_1^* = N_{av}$, $E = N_E - E^* - S_1^* = N_{av}^E$, where $N$ and $N_E$ are the total amounts of subunits and enzymes, respectively.

***Model results and predictions.*** Using the above described dynamics (Eqs. 2-4 and Fig. 3B), we performed stochastic simulations of a pair of centrosomes growing from a shared pool of enzymes and subunits. The resulting growth dynamics is sigmoidal, and lead to equally sized centrosomes (Fig. 3C). Interestingly, the dynamics of the activated enzyme show an *activation pulse* at the onset of growth (Fig. 3C). This pulse in the cytoplasmic concentration of active enzymes arises from the dynamics of enzyme activation by the PCM scaffold and its subsequent consumption by PCM subunits. The amplitude and the lifetime of the pulse depend on the difference in the timescales of enzyme activation and consumption (Fig. S4). Notably, a pulse of Polo kinase has been observed to initiate centrosome assembly in *Drosophila* (28). The experimentally observed Polo pulse is regulated by the abundance of the centriolar protein Ana1 (28), which controls the enzyme activation rate ($k_E^*$ in our model). Exploring the effect of the enzyme activation rate $k_E^*$, we observe increased pulse period and decreased pulse amplitude with decreasing enzyme activation rate (Fig. S4). These results are similar to the experimentally observed effect of reduced Ana1, which reduces the overall rate of Polo activation in the centrosome (28).

Importantly, this model ensures robustness in centrosome size equality, with a negligible difference in steady-state size ($\sim 2\%$ of mean size) that is independent of the initial size difference (Fig. 3D). The difference in steady-state size is a result of the fluctuations in the individual centrosome size dynamics, as evident from the distribution of the size difference (Fig. 3D-inset). We find that the centrosome growth dynamics predicted by this model match really well with the experimental growth curves in *C. elegans* (13) (Fig. 3E).

Though centrosome growth in *C. elegans* is found to be sigmoidal, it has been suggested that centrosomes in *Drosophila* grow in a non-sigmoidal fashion (8). Although we could not find any direct quantitative measurement of centrosome size dynamics in *Drosophila* or other organisms, analysis of PCM assembly dynamics using flourescence reporters show

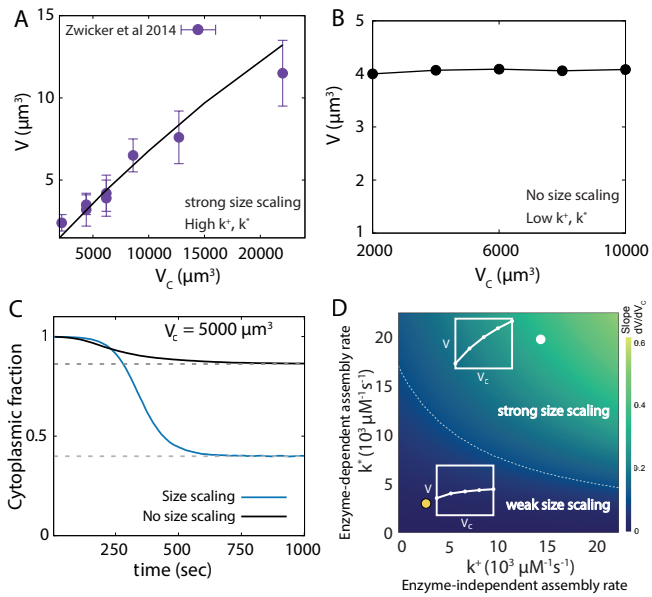


**Fig. 4. Centrosome size scaling with cell size.** (A) Scaling of centrosome size with cell size obtained from the catalytic growth model (line) fitted to experimental data (points) in *C. elegans* embryo (8). (B) Centrosome size does not scale with cell size when the assembly rates are much lower compared to disassembly rate (i.e., $k^*, k^+ \lesssim k^- V_c$). (C) Dynamics of the cytoplasmic fraction of subunits ($S_1$ and $S_1^*$ combined) reveal significantly higher pool depletion in the size scaling regimes. The two curves correspond to the growth curves shown in panels A (blue) and B (black). The dashed lines are theoretical results obtained from the deterministic model. (D) An analytically obtained phase diagram of centrosome size scaling as functions of enzyme-dependent and enzyme-independent assembly rate constants. The color indicates the strength of size scaling (measured by $dV/dV_c$). The dashed gray line indicates the contour $dV/dV_c = 0.1$. Here the slope values are shown in $\delta v$ units. Insets: Characteristic size scaling behaviours. See Table 1 for a list of parameter values.

varying degrees of cooperativity during *Drosophila* development (28). We therefore sought to explore whether our catalytic growth model can also describe non-sigmoidal growth. To this end, we characterized the sigmoidal nature of the growth by fitting the dynamics of centrosome volume $V(t)$ to a Hill function of the form $At^\alpha/(B^\alpha + t^\alpha)$, where the coefficient $\alpha$ represents the strength of cooperativity. Our results show that the cooperative nature of growth depends on the interplay between the growth rate constant $k^+$ and the total enzyme concentration $[E]$, such that growth is sigmoidal ($\alpha \geq 2$) for larger $[E]$ and smaller $k^+$, and non-sigmoidal otherwise (Fig. 3F).

While our model of shared catalysis considers a limiting pool of enzymes, a finite enzyme pool is not required for robust size control. To show this, we considered an unlimited pool inactive enzymes ($E$), such that the cytoplasmic concentration of $E$ does not change over time (Fig. 3G). The unlimited pool of inactive enzymes keeps producing activated enzymes via the centrosomes. The centrosome size reaches a steady-state when the subunit activation (via $E^*$) and subsequent growth is balanced by subunit disassembly from the centrosome (Fig. 3G-inset). The size equality and cooperativity of growth remain intact in the presence of constant $[E]$ (Fig. 3H). The prevalence of activated enzyme almost entirely depletes the inactive subunit pool and the centrosomes are in chemical equilibrium with the active subunit pool in the steady state (Fig. 3H-inset).

### Cytoplasmic pool depletion regulates centrosome size scaling with cell size.

Since our model for centrosome growth is limited by a finite amount of subunits, it is capable of capturing centrosome size scaling with cell size (Fig. 4A), in excellent agreement with experimental data (8, 13). However, the extent of organelle size scaling with cell size depends on the assembly rate and becomes negligible when the assembly rate is not significantly higher compared to the disassembly rate (Fig. 4B). In particular, centrosome size scaling is connected to the extent of subunit pool depletion, such that the steady-state cytoplasmic fraction of the subunits is low when centrosome size scales with the cell size and higher otherwise (Fig. 4C).

To understand how size scaling is regulated by growth parameters, we derived a simplified analytical form (see SI section III) for the steady-state centrosome size given by

$$V = \frac{(E^* k_1^* + k^+) k^* \rho_0 V_c \delta v}{k^*(k^+ + k^- V_c) + E^* k_1^* (k^* + k^- V_c)}, \qquad \textbf{(5)}$$

where $\delta v$ is the volume occupied by a centrosome subunit, $\rho_0$ is the total subunit density, and the enzymes are assumed to reach their steady-state abundance $E^*$ very fast. From the above expression, we can see that centrosome size $V$ will strongly scale with cell size $V_c$ when $k^+, k^* \gg k^- V_c$. This result is reflected in the phase diagram of size scaling (measured as the slope $\sim \mathrm{d}V/\mathrm{d}V_c$), which shows stronger size scaling with increasing assembly rates (Fig. 4D). The subunit pool depletion also increases with the assembly rates, reaching a state of almost complete depletion (i.e., $V \to \rho_0 V_c \delta v$) as we approach the regime of strong size scaling (see Fig. S5).

It is important to note here that size scaling with cell size reported here is different from the linear size scaling predicted by the canonical limiting pool model (13, 18). Robust size control for multiple centrosomes requires size-dependent negative feedback and with this feedback, the size scaling with cell size becomes a feature achieved in a range of cell volumes by tuning growth rates. Interestingly, strong size scaling has been observed in *C. elegans* embryos (13), which are smaller in size ($\sim 10^4\,\mu\mathrm{m}^3$) than Drosophila embryos ($\sim 10^6\,\mu\mathrm{m}^3$) that do not exhibit size scaling with centrosome number (inferred from intensity data in (28)). This feature can be explained by our model in the regime of weaker size scaling, which is expected for larger system sizes (see SI section III & Fig. S5). Thus, the parameters of our model can be tuned to capture both sigmoidal and non-sigmoidal growth and strong or weak size scaling, without changing the nature of the molecular interactions that are largely conserved across organisms (24).

### Control of centrosome size asymmetry through differential growth.

An essential aspect of centrosome size regulation is the modulation of centrosome size by centriole activity. In particular, it has been shown that the centrosome associated

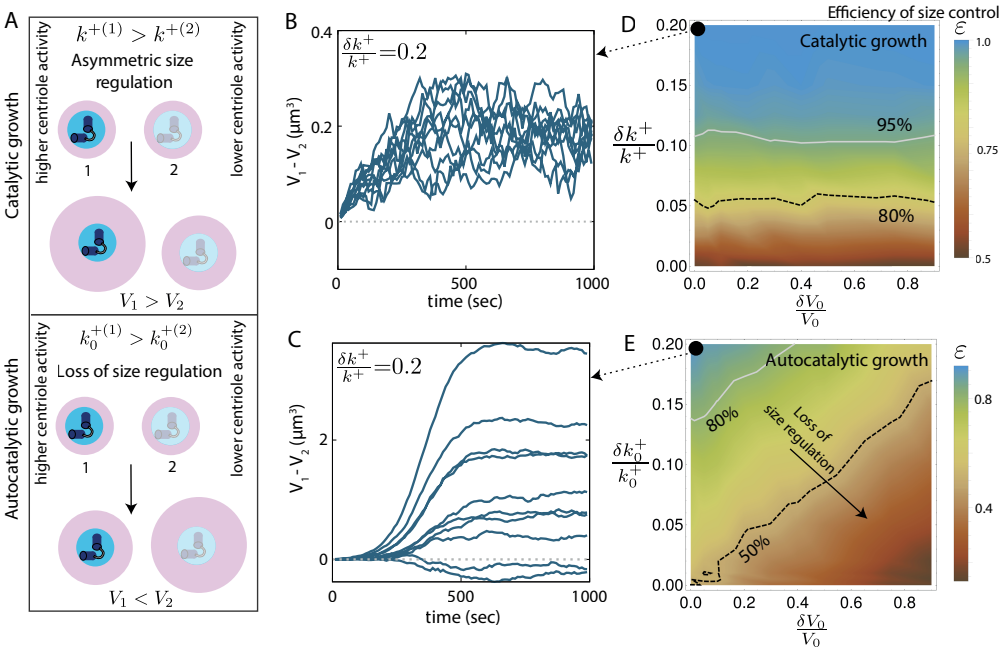


**Fig. 5. Control of centrosome size asymmetry via differential growth.** (A) Schematic illustrating asymmetric size regulation via differential growth in the (top) catalytic growth model and (bottom) autocatalytic growth model. (B,C) Ten representative trajectories showing the dynamics of centrosome size difference ($V_1 - V_2$) for (B) catalytic growth model ($\delta k^+/k^+ = 0.2$), and (C) autocatalytic growth model ($\delta k_0^+/k_0^+ = 0.2$). The two centrosomes are initially of the same size. (D) Efficiency growth-rate-dependent control of centrosome size asymmetry ($\varepsilon = N^+/N_{\text{tot}}$) as a function of (normalized) initial size difference ($\delta V_0/V_0$) and (normalized) growth rate difference ($\delta k^+/k^+$), in the catalytic growth model. (E) Efficiency of growth-rate-dependent control of centrosome size asymmetry as a function of (normalized) initial size difference ($\delta V_0/V_0$) and (normalized) growth rate difference ($\delta k_0^+/k_0^+$), in the autocatalytic growth model. See Table 1 for a list of model parameters.

with a more active centriole will grow larger, resulting in centrosomes of unequal size (25, 26). Control of centriole activity-driven centrosome size asymmetry is important as this size asymmetry may play a crucial role in stem cell division as observed in *Drosophila* neuroblasts (25). We test the effectiveness of size regulation by studying the growth of a centrosome pair with different centriole activities, controlled by the values of the growth rate constants $k_0^+$ and $k^+$ for the autocatalytic (Eq. 1) and the catalytic (Fig. 3B) growth models, respectively (Fig. 5A). For both the models, we bias the initial size of the centrosomes by assigning a smaller initial size ($V_0 - \delta V_0$) to the centrosome with a higher centriole activity (i.e., $k_0^{+(1)} = k_0^+ + \delta k_0^+$ or $k^{+(1)} = k^+ + \delta k^+$). We then simulate the growth of $N_{\text{tot}}$ centrosome pairs and quantify the efficiency ($\varepsilon$) of size control as the ratio of the number of cases ($N^+$) where the centrosome with higher growth rate ($k_0^+ + \delta k_0^+$ or $k^+ + \delta k^+$) becomes larger, to the total number of simulated pairs, $\varepsilon = N^+/N_{\text{tot}}$.

In the absence of any initial size difference ($\delta V_0 = 0$), the catalytic growth model shows better control of differential growth-induced size asymmetry (Fig. 5B), while the autocatalytic growth model shows wide variations in centrosome size difference (Fig. 5C). We find that the catalytic growth model ensures that the centrosome with a larger $k^+$ (higher centriole activity) end up being larger, irrespective of the initial size difference (Fig. 5D). This illustrates robust control of centrosome size asymmetry by controlling differences in centriole activity. By contrast, in the autocatalytic growth model, the efficiency of size control monotonically decreases with increasing initial size difference, reflecting the lack of robustness in size control (Fig. 5E).

### Multi-component centrosome model reveals the utility of shared catalysis on centrosome size control.

One major postulate of the one-component PCM model was that the enzyme pool was shared between the two centrosomes rather than being localized to each. Here we support this assumption using a multi-component centrosome model that allows us to model the specific interactions between the enzyme and the centrosome components. Based on recent studies (9, 10), we model the centrosomes with two essential scaffold-forming proteins, $a$ and $b$, whose assembly into the PCM scaffold is regulated by the kinase $E$. The total size of the PCM scaffold, $S$, and the centrosome volume $V$ are given by $S = S(a) + S(b)$ and $V = V_a + V_b$, where $S(a)$ ($S(b)$) and $V_a$ ($V_b$) denote the contribution to the scaffold size (in number of subunits) and the centrosome volume by the component $a$ ($b$). The molecular identities of these key components are listed in Table 2 for different organisms. In particular, for *Drosophila*, $a$ and $b$ can be identified as the scaffold forming proteins Spd-2 and Cnn, while $E$ represents the kinase Polo. It has been observed that Spd-2 and Cnn cooperatively form the PCM scaffold to recruit almost all other proteins involved in centrosome maturation (7). To effectively coordinate cooperative growth of the scaffold, Spd-2 proteins recruit the kinase Polo, which in turn phosphorylates Cnn at the centrosome (9). In the absence of Polo, Cnn proteins can bind to the scaffold but fall off rapidly, leading to diminished centrosome maturation (9, 29).

We incorporated these experimental observations in our

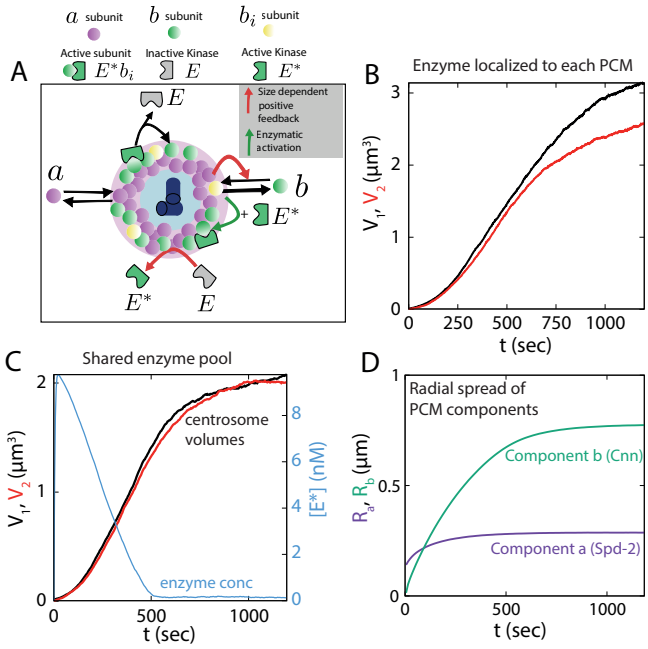


**Fig. 6. Multi-component model for centrosome growth.** (A) Schematic of centrosome growth model driven by two scaffold components $a$ and $b$, and enzyme E. $a$ can bind the existing PCM independent of $b$ or the enzyme $E$. The enzyme is activated by $a$ in the scaffold, then released in the cytoplasm as $E^*$. The other scaffold former $b$ binds to PCM in $a$-dependent manner in an intermediate form $b_i$ which can undergo rapid disassembly. The intermediate form $b_i$ can get incorporated in the $b$-scaffold by the active enzyme $E^*$ via forming an activated subunit form $E^*b_i$. The red arrows indicate the size dependent positive feedback and the green arrow indicates the catalytic activity of the enzyme. (B) Centrosome size $(V_1, V_2)$ dynamics for growth with localized enzyme. (C) Centrosome size $(V_1, V_2)$ dynamics for growth with shared enzyme pool (black and red curve) and the pulse-like dynamics of activated enzyme concentration ($[E^*]$, blue curve). (D) Radial spread of the two scaffold former components $a$ and $b$ corresponding to the centrosome growth shown in panel-C. See Table 1 for a list of parameter values.

multi-component model as described in Fig. 6A. We then test two different models for enzyme spatial distribution: (i) enzyme $E$ (Polo) is activated at each centrosome by the scaffold component $a$ (Spd-2), which then assembles the second component $b$ (Cnn) into the scaffold of that particular centrosome (for details see SI Section IVA), and (ii) enzyme $E$ activated by the scaffold component $a$ is released in the cytoplasmic pool, promoting assembly of the $b$-scaffold at both centrosomes (for details see SI Section IVB). In the first case, localized enzyme interaction exclusively enhances the growth of the individual centrosomes, creating an autocatalytic feedback that leads to size inequality of centrosomes (Fig. 6B). Similar to model Eq. (1), the steady-state size difference between the two centrosomes increases with the increasing initial size difference, resulting in a failure of robust size control (Fig. S6).

We then considered the second case where the enzyme-mediated catalysis is shared between the growing centrosome pair. Experimental observations suggest a dynamic enzyme population around the centrosomes (19, 30), with a turnover timescale much smaller than the scaffold forming proteins (7, 31). These findings point towards the possibility that the enzyme is transiently localized in the centrosome during activation and the active enzyme is then released in the cytoplasmic pool that can enhance the growth of both the centrosomes (Fig. 6A). We incorporate this shared catalysis mechanism in the second model where $a$ activates the enzyme to $E^*$ which then gets released in the cytoplasm, facilitating $b$-scaffold expansion in both the centrosomes (see SI Section IVB for details). This growth mechanism is able to robustly control centrosome size equality (Fig. S7), giving rise to the characteristic sigmoidal growth dynamics (Fig. 6C), where the first scaffold former $a$ is smaller in amount than the second, enzyme-aided component $b$. This difference in the abundances of $a$ and $b$ proteins, when translated into their respective radial spread from the centrosome center ($R \propto V^{1/3}$), bears close resemblance with the relative spread in Spd-2 and Cnn observed in the experiments, where the Cnn spread is twice as large as Spd-2 (7, 9) (Fig. 6D). The active enzyme dynamics also resembles the observed pulse in Polo dynamics at the beginning of centrosome maturation (28) (Fig. 6C). Overall, the two-component model provides crucial insights into the role of shared catalytic growth on centrosome size control and lays the theoretical foundation for further investigations into the molecular processes that govern centrosome assembly.

## Discussion

***Autocatalytic feedback drives centrosome size inequality.*** In this article, we examined quantitative models for centrosome growth via assembly and disassembly of its constituent building blocks to understand how centrosome size is regulated during maturation. Although there is no generally accepted model for centrosome size regulation, previous studies (7–10, 29, 32) have suggested that centrosome assembly is cooperative and driven by a positive feedback mechanism. It has been quantitatively shown that an autocatalytic growth model (8) captures the cooperative growth dynamics of individual centrosomes as well as their size scaling features. However, as we showed here, autocatalytic growth does not guarantee the size equality of two centrosomes growing from a shared subunit pool. The resultant size inequality increases with the initial size difference between the centrosomes, indicating a lack of robustness in size control. This observation remains valid even within models where autocatalysis is not explicitly invoked, but emerges from positive feedback between PCM components (9). For instance, the positive feedback between Spd-2 and Cnn within Drosophila centrosomes results in the accumulation of more Cnn where Spd-2 is abundant. This, in turn, amplifies the retention of Spd-2 and binding of Cnn, culminating in a size-dependent positive feedback (akin to autocatalytic feedback) in PCM assembly. Given the current molecular understanding, it remains an open question whether localized assembly around the centriole, driven by autocatalytic feedback, is sufficient to furnish a robust mechanism for centrosome size regulation.

***Model of centrosome pair growth via shared catalysis.*** Following recent experiments on the molecular mechanisms governing centrosome assembly, we constructed an enzyme-mediated catalytic growth model that not only describes cooperative growth behavior but also ensures robustness in

size equality of the two maturing centrosomes. The enzyme Polo-like kinase (PLK1) that coordinates centrosome growth (9, 29, 32, 33), gets phosphorylated in the centrosome and has a much faster turnover rate than the centrosome scaffold forming proteins Spd-2 and Cnn (7, 31). Experimentally observed PLK1 diffusivity of $\sim 5\ \mu\text{m}^2 s^{-1}$ (19) also indicates that PLK1 transfer between the centrosome pair (assuming at a distance of $\sim 5 - 10\ \mu$m) may occur within 5-20 seconds which is much faster than the timescale of centrosome growth ($\sim 1000$ sec). This indicates that the kinase dynamics is not diffusion-limited, consistent with recent studies reporting negligible gradient in cytoplasmic Polo in *C elegans* embryo (34). These insights led us to hypothesize that the kinase, once activated at the centrosome, could be released into the cytoplasm, becoming part of a shared pool of enzymes. This pool would then catalyze the growth of both centrosomes without any inherent bias. While we theoretically demonstrated that this mechanism of shared catalysis can robustly regulate centrosome size, it is important to acknowledge that the specific predictions concerning enzyme dynamics can only be validated through further experiments.

***Localized catalysis leads to centrosome size disparity.*** To further explore the role of enzymes in mediating centrosome growth and predict the consequence of an enzyme pool that is not shared equally by the two centrosomes, we extended our single-component model of catalytic growth to a multi-component model. This extended model incorporates the interactions PCM scaffold-forming proteins (Spd-2 and Cnn in Drosophila) and the enzyme Polo kinase. Using this model, we showed that localized catalysis by the enzyme—indicative of an unshared pool—leads to significqnt size differences in the centrosomes. While direct experimental validation of a shared enzyme pool remains outstanding, it is intriguing to consider the findings that a centrosome-anchored Plk1 construct (Plk1-AKAP) induces anomalous centrosome maturation and defective spindle formation (30).

***Enzyme-mediated size control.*** Our findings reveal that centrosome size increases with increasing enzyme concentration and that centrosome growth is inhibited in the absence of the enzyme (Fig. S7). Since the activity of the Polo kinase is cell-cycle dependent (35, 36), we further explored the dynamics of centrosome growth with a time-dependent dynamics of the enzyme. We found that centrosome growth can be triggered by switching on the enzyme dynamics and centrosome size was reduced when the enzyme was switched off (Fig. S7). Importantly, it supported the experimental observation that a continuous Polo activity is required to maintain the PCM scaffold (19, 37). Many key features of centrosome growth such as the sigmoidal growth curve and size scaling behavior can be modulated in our model by changing the growth rate constants and enzyme concentration, while conserving the underlying molecular mechanisms for assembly. This opens up the possibility that the catalytic growth model may be broadly relevant to other organisms where homologous proteins (Table 2) play similar functional roles in regulating centrosome growth (10).

***Testable model predictions.*** Aside from capturing the existing data on the dynamics of centrosome growth, our catalytic growth model makes several specific predictions that can be tested in future experiments. Firstly, our model posits the sharing of the enzyme between both centrosomes. This hypothesis can potentially be experimentally tested through immunofluorescent staining of the kinase or by constructing FRET reporter of PLK1 activity. It is important to to acknowledge that while we exclusively focused on Polo kinase as the sole enzyme, this shared catalytic activity might also involve other molecular players that interact with Polo, such as cyclin B/Cdk1 (30). Moreover, our model provides explicit predictions regarding the enzyme's role in influencing centrosome size and growth. These predictions encompass the anticipated increase in centrosome size with increasing enzyme concentration, the ability to modify the shape of the sigmoidal growth curve, and the manipulation of centrosome size scaling patterns by perturbing growth rate constants or enzyme concentrations. Additionally, the model suggests inducing a shift from strong size scaling to weak size scaling through the reduction of PCM assembly rate or via cytoplasmic subunit pool depletion.

Secondly, an intriguing implication of our model is the robust regulation of centrosome size through catalytic PCM assembly during maturation. One direct avenue for testing this result is to observe the dynamics of two initially unequal-sized centrosomes during the early maturation phase. The catalytic growth model predicts that the final size difference of the centrosomes will remain independent of their initial size disparity. This prediction can be experimentally examined by inducing varying centrosome sizes at the early stage of maturation. Experimentally validating these predictions will play a pivotal role in building a quantitative understanding of centrosome size regulation during mitosis.

## References


1. Roy R Gould and Gary G Borisy. The pericentriolar material in chinese hamster ovary cells nucleates microtubule formation. *The Journal of cell biology*, 73(3):601–615, 1977.
2. Robert E Palazzo, Jacalyn M Vogel, Bradley J Schnackenberg, Dawn R Hull, and Xingyong Wu. Centrosome maturation. *Current topics in developmental biology*, 49:449–470, 1999.
3. A Krämer, K Neben, and AD Ho. Centrosome replication, genomic instability and cancer. *Leukemia*, 16(5):767–775, 2002.
4. Antonino B D'Assoro, Wilma L Lingle, and Jeffrey L Salisbury. Centrosome amplification and the development of cancer. *Oncogene*, 21(40):6146–6153, 2002.
5. Renata Basto, Kathrin Brunk, Tatiana Vinadogrova, Nina Peel, Anna Franz, Alexey Khodjakov, and Jordan W Raff. Centrosome amplification can initiate tumorigenesis in flies. *Cell*, 133(6):1032–1042, 2008.
6. Michelle S Levine, Bjorn Bakker, Bram Boeckx, Julia Moyett, James Lu, Benjamin Vitre, Diana C Spierings, Peter M Lansdorp, Don W Cleveland, Diether Lambrechts, et al. Centrosome amplification is sufficient to promote spontaneous tumorigenesis in mammals. *Developmental cell*, 40(3):313–322, 2017.
7. P T Conduit, Jennifer H Richens, Alan Wainman, James Holder, Catarina C Vicente, Metta B Pratt, Carly I Dix, Zsofia A Novak, Ian M Dobbie, Lothar Schermelleh, and Jordan W Raff. A molecular mechanism of mitotic centrosome assembly in drosophila. *eLife*, 3(e03399), 2014.
8. D Zwicker, M Decker, S Jaensch, A A Hyman, and F Jülicher. Centrosomes are autocatalytic droplets of pericentriolar material organized by centrioles. *Proc Natl Acad Sci*, 111:E2636–2645, 2014.
9. Ines Alvarez-Rodrigo, Thomas L Steinacker, Saroj Saurya, Paul T Conduit, Janina Baumbach, Zsofia A Novak, Mustafa G Aydogan, Alan Wainman, and Jordan W Raff. Evidence that a positive feedback loop drives centrosome maturation in fly embryos. *Elife*, 8, 2019.
10. Paul T Conduit, Alan Wainman, and Jordan W Raff. Centrosome function and assembly in animal cells. *Nature reviews Molecular cell biology*, 16(10):611–624, 2015.
11. Bradley J Schnackenberg, Alexey Khodjakov, Conly L Rieder, and Robert E Palazzo. The disassembly and reassembly of functional centrosomes in vitro. *Proceedings of the National Academy of Sciences*, 95(16):9295–9300, 1998.
12. Zhe Feng, Anna Caballe, Alan Wainman, Steven Johnson, Andreas F.M. Haensele,

Matthew A. Cottee, Paul T. Conduit, Susan M. Lea, and Jordan W. Raff. Structural basis for mitotic centrosome assembly in flies. *Cell*, 169:1078–1089, 2017.
13. Markus Decker, Steffen Jaensch, Andrei Pozniakovsky, Andrea Zinke, Kevin F. O'Connell, Wolfgang Zachariae, Eugene Myers, and Anthony A. Hyman. Limiting amounts of centrosome material set centrosome size in c. elegans embryos. *Current Biology*, 21(6):1259–1267, 2011.
14. J. B. Woodruff, O. Wueseke, and A. A. Hyman. Pericentriolar material structure and dynamics. *Philos. Trans. R. Soc. Lond.*, B 369(20130459), 2014.
15. C.A. Kemp, K.R. Kopish, P. Zipperlen, J. Ahringer, and K.F. O'Connell. Centrosome maturation and duplication in c. elegans require the coiled-coil protein spd-2. *Dev. Cell*, 6:511–523, 2004.
16. L. Pelletier, N. Ozlü, E. Hannak, C. Cowan, B. Habermann, M. Ruer, T. Müller-Reichert, and A.A. Hyman. The caenorhabditis elegans centrosomal protein spd-2 is required for both pericentriolar material recruitment and centriole duplication. *Curr. Biol.*, 14:863–873, 2004.
17. Garrett Greenan, Clifford P Brangwynne, Steffen Jaensch, Jöbin Gharakhani, Frank Jülicher, and Anthony A Hyman. Centrosome size sets mitotic spindle length in caenorhabditis elegans embryos. *Current Biology*, 20(4):353–358, 2010.
18. Nathan W Goehring and Anthony A Hyman. Organelle growth control through limiting pools of cytoplasmic components. *Curr. Biol.*, 22(9):R330–R339, 2012.
19. Robert Mahen, Anand D Jeyasekharan, Nicholas P Barry, and Ashok R Venkitaraman. Continuous polo-like kinase 1 activity regulates diffusion to maintain centrosome self-organization during mitosis. *Proceedings of the National Academy of Sciences*, 108(22): 9310–9315, 2011.
20. Robert Mahen and Ashok R Venkitaraman. Pattern formation in centrosome assembly. *Current opinion in cell biology*, 24(1):14–23, 2012.
21. P T Conduit, K Brunk, J Dobbelaere, C I Dix, E P Lucas, and J W Raff. Centrioles regulate centrosome size by controlling the rate of cnn incorporation into the pcm. *Curr. Biol*, 20: 2178–2186, 2010.
22. M Kirkham, T Müller-Reichert, K Oegema, S Grill, and A A Hyman. Sas-4 is a c. elegans centriolar protein that controls centrosome size. *Cell*, 112(4):575–587, 2003.
23. Deb Sankar Banerjee and Shiladitya Banerjee. Size regulation of multiple organelles competing for a limiting subunit pool. *PLOS Computational Biology*, 18(6):e1010253, 2022.
24. Jordan W Raff. Phase separation and the centrosome: a fait accompli? *Trends in Cell Biology*, 2019.
25. Paul T Conduit and Jordan W Raff. Cnn dynamics drive centrosome size asymmetry to ensure daughter centriole retention in drosophila neuroblasts. *Current Biology*, 20(24):2187–2192, 2010.
26. J Januschke, J Reina, S Llamazares, T Bertran, F Rossi, J Roig, and C Gonzalez. Centrobin controls mother–daughter centriole asymmetry in drosophila neuroblasts. *Nature cell biology*, 15(3):241–248, 2013.
27. Jeroen Dobbelaere, Filipe Josue, Saskia Suijkerbuijk, Buzz Baum, Nicolas Tapon, and Jordan Raff. A genome-wide rnai screen to dissect centriole duplication and centrosome maturation in drosophila. *PLoS biology*, 6(9):e224, 2008.
28. Siu-Shing Wong, Zachary M Wilmott, Saroj Saurya, Ines Alvarez-Rodrigo, Felix Y Zhou, Kwai-Yin Chau, Alain Goriely, and Jordan W Raff. Centrioles generate a local pulse of polo/plk1 activity to initiate mitotic centrosome assembly. *The EMBO Journal*, 41(11): e110891, 2022.
29. Jeffrey B Woodruff, Oliver Wueseke, Valeria Viscardi, Julia Mahamid, Stacy D Ochoa, Jakob Bunkenborg, Per O Widlund, Andrei Pozniakovsky, Esther Zanin, Shirin Bahmanyar, et al. Regulated assembly of a supramolecular centrosome scaffold in vitro. *Science*, 348(6236): 808–812, 2015.
30. Kazuhiro Kishi, Marcel ATM Van Vugt, Ken-ichi Okamoto, Yasunori Hayashi, and Michael B Yaffe. Functional dynamics of polo-like kinase 1 at the centrosome. *Molecular and cellular biology*, 29(11):3134–3150, 2009.
31. Paul T Conduit, Alan Wainman, Zsofia A Novak, Timothy T Weil, and Jordan W Raff. Re-examining the role of drosophila sas-4 in centrosome assembly using two-colour-3d-sim frap. *Elife*, 4:e08483, 2015.
32. Paul T Conduit, Zhe Feng, Jennifer H Richens, Janina Baumbach, Alan Wainman, Suruchi D Bakshi, Jeroen Dobbelaere, Steven Johnson, Susan M Lea, and Jordan W Raff. The centrosome-specific phosphorylation of cnn by polo/plk1 drives cnn scaffold assembly and centrosome maturation. *Developmental cell*, 28(6):659–669, 2014.
33. Midori Ohta, Zhiling Zhao, Di Wu, Shaohe Wang, Jennifer L Harrison, J Sebastián Gómez-Cavazos, Arshad Desai, and Karen F Oegema. Polo-like kinase 1 independently controls microtubule-nucleating capacity and size of the centrosome. *Journal of Cell Biology*, 220 (2), 2021.
34. Sofia Barbieri, Aparna Nurni Ravi, Erik E Griffin, and Monica Gotta. Modeling protein dynamics in caenorhabditis elegans embryos reveals that the plk-1 gradient relies on weakly coupled reaction–diffusion mechanisms. *Proceedings of the National Academy of Sciences*, 119(11):e2114205119, 2022.
35. Ryoji Hamanaka, Mark R Smith, Patrick M O'Connor, Sharon Maloid, Kelly Mihalic, Jerry L Spivak, Dan L Longo, and Douglas K Ferris. Polo-like kinase is a cell cycle-regulated kinase activated during mitosis. *Journal of Biological Chemistry*, 270(36):21086–21091, 1995.
36. Takeshi Uchiumi, Dan L Longo, and Douglas K Ferris. Cell cycle regulation of the human polo-like kinase (plk) promoter. *Journal of Biological Chemistry*, 272(14):9166–9174, 1997.
37. Gabriela Cabral, Triin Laos, Julien Dumont, and Alexander Dammermann. Differential requirements for centrioles in mitotic centrosome growth and maintenance. *Developmental Cell*, 50(3):355–366, 2019.
38. Daniel T Gillespie. Exact stochastic simulation of coupled chemical reactions. *The Journal of Physical Chemistry*, 81(25):2340–2361, 1977.
39. Danielle R Hamill, Aaron F Severson, J Clayton Carter, and Bruce Bowerman. Centrosome maturation and mitotic spindle assembly in c. elegans require spd-5, a protein with multiple coiled-coil domains. *Developmental cell*, 3(5):673–684, 2002.
40. Hannes Fischer, Igor Polikarpov, and Aldo F Craievich. Average protein density is a molecular-weight-dependent function. *Protein Science*, 13(10):2825–2828, 2004.
41. Oliver Wueseke, David Zwicker, Anne Schwager, Yao Liang Wong, Karen Oegema, Frank Jülicher, Anthony A Hyman, and Jeffrey B Woodruff. Polo-like kinase phosphorylation determines caenorhabditis elegans centrosome size and density by biasing spd-5 toward an assembly-competent conformation. *Biology Open*, 5(10):1431–1440, 2016.
42. Maria Ana Gomez-Ferreria, Uttama Rath, Daniel W Buster, Sumit K Chanda, Jeremy S Caldwell, Daniel R Rines, and David J Sharp. Human cep192 is required for mitotic centrosome and spindle assembly. *Current Biology*, 17(22):1960–1966, 2007.
43. Ka-Wing Fong, Yuk-Kwan Choi, Jerome B Rattner, and Robert Z Qi. Cdk5rap2 is a pericentriolar protein that functions in centrosomal attachment of the $\gamma$-tubulin ring complex. *Molecular biology of the cell*, 19(1):115–125, 2008.
44. Heidi A Lane and Erich A Nigg. Antibody microinjection reveals an essential role for human polo-like kinase 1 (plk1) in the functional maturation of mitotic centrosomes. *The Journal of cell biology*, 135(6):1701–1713, 1996.

## Methods

**Stochastic growth simulations**. We use the Gillespie algorithm (38) to simulate the stochastic growth of one or multiple structures from a common pool of subunits. At any time $t$ the Gillespie algorithm uses two random variables drawn from an uniform distribution ($r_1, r_2 \in \mathcal{U}(0,1)$), and the instantaneous propensities for all of the possible reactions to update the system in time according to the defined growth law. The propensities of the relevant reactions, i.e., the assembly and disassembly rates of the $i^{th}$ structure are given by $K_i^{\text{on}}$ and $K_i^{\text{off}}$ respectively. For our growth model these propensities are functions of subunit pool size ($N$) and structure size ($n_i$),

$$K_i^{\text{on}} = k^+ \left( \frac{N - \sum_{i=1}^{M} n_i}{V} \right) , \quad \textbf{(6)}$$

$$K_i^{\text{off}} = k^- n_i^{\beta} , \quad \textbf{(7)}$$

where we are considering growth of $M$ structures from a shared pool. The Gillespie algorithm computes the time for the next reaction at $t+\tau$ given the current state of the system (i.e., the propensities for all reactions) at time $t$ where $\tau$ is given by-

$$\tau = \frac{1}{\sum_{i=1}^{C} \mathcal{R}_i} \log \left( \frac{1}{r_1} \right) , \quad \textbf{(8)}$$

where $\mathcal{R}_i$ is the propensity of $i^{th}$ reaction and $C$ is the total number of all possible reactions. The second random variable $r_2$ is used to select the particular reaction ($j^{th}$ reaction) that will occur at $t+\tau$ time such that

$$\frac{\sum_{i=1}^{j-1} \mathcal{R}_i}{\sum_{i=1}^{C} \mathcal{R}_i} \leq r_2 < \frac{\sum_{i=1}^{j} \mathcal{R}_i}{\sum_{i=1}^{C} \mathcal{R}_i} . \quad \textbf{(9)}$$

The condition for the first reaction ($j = 1$) is $0 \leq r_2 < \frac{\mathcal{R}_1}{\sum_{i=1}^{C} \mathcal{R}_i}$. The two steps defined by Eq. 8 and Eq. 9 are used recursively to compute the growth dynamics in time.

**Subunit size estimation**. Though we use single subunit and two subunit models of growth, we have used same value for the volume occupied by the subunit $\delta v$. We estimate the value of $\delta v$ from the molecular weight of SPD-5 which is 135 kDa (39). Taking the protein mass density to be $1.4$ gcc$^{-1}$ (40) and the PCM volume fraction to be $\sim 0.1$ (19), we estimate the volume occupied by SPD-5 in PCM to be $0.1 \times 162 \times 10^{-7}\,\mu\text{m}^3 \sim 2 \times 10^{-4}\,\mu\text{m}^3$.

## Acknowledgements

We thank Jordan Raff and Zachary Wilmott for many useful discussions. SB acknowledges support from the National Institutes of Health (NIH R35 GM143042) and the David Scaife Foundation.

## Acknowledgements

SB and DSB designed and developed the theory. DSB performed numerical simulations and analyzed the data. DSB and SB wrote the paper.

**Table 1.** Parameter values

| Figure | Parameter Values |
|---|---|
| Fig. 1C | $\rho_0(=N/V_c)$=0.033 $\mu$M, $k_0^+$= 600 $\mu\text{M}^{-1}\,s^{-1}$, $k_1^+$= 0.6 $\mu\text{M}^{-1}\,s^{-1}$ |
| Fig. 2A | $\rho_0$=0.033 $\mu$M |
| Fig. 2D | $k^+$=1000 $\mu\text{M}^{-1}\,s^{-1}$, $\rho_0$=0.1 $\mu$M |
| Fig. 3C | $\rho_0$ = 1 $\mu$M, $[E]$ = 0.1 $\mu$M, $k^+ = 1\,\mu\text{M}^{-1}s^{-1}$, $k^* = 1000\,\mu\text{M}^{-1}s^{-1}$, $k_E^* = 5\,s^{-1}$, $k_1^* = 1\,\mu\text{M}^{-1}s^{-1}$ |
| Fig. 3D | $\rho_0$ = 0.05 $\mu$M, $[E]$ = 0.1 $\mu$M, $k^+ = 1\,\mu\text{M}^{-1}s^{-1}$, $k^* = 2000\,\mu\text{M}^{-1}s^{-1}$, $k_E^* = 10\,s^{-1}$, $k_1^* = 100\,\mu\text{M}^{-1}s^{-1}$ |
| Fig. 3E | $\rho_0$ = 0.02 $\mu$M, $[E]$ = 0.09 $\mu$M, $k^+ = 1\,\mu\text{M}^{-1}s^{-1}$, $k^* = 8\times10^4\,\mu\text{M}^{-1}s^{-1}$, $k_E^* = 4.25\,s^{-1}$, $k_1^* = 0.1\,\mu\text{M}^{-1}s^{-1}$ |
| Fig. 3F | $\rho_0$ = 1 $\mu$M, $k^* = 1000\,\mu\text{M}^{-1}s^{-1}$, $k_E^* = 5\,s^{-1}$, $k_1^* = 10\,\mu\text{M}^{-1}s^{-1}$ |
| Fig. 3G & H | $\rho_0$ = 0.15 $\mu$M, $[E]$ = 0.085 $\mu$M, $k^+ = 1\,\mu\text{M}^{-1}s^{-1}$, $k^* = 1000\,\mu\text{M}^{-1}s^{-1}$, $k_E^* = 1\,s^{-1}$, $k_1^* = 5\,\mu\text{M}^{-1}s^{-1}$ |
| Fig. 4A | Same as Fig. 3E |
| Fig. 4B | $\rho_0$ = 0.1 $\mu$M, $[E]$ = 0.05 $\mu$M, $k^+ = 100\,\mu\text{M}^{-1}s^{-1}$, $k^* = 2000\,\mu\text{M}^{-1}s^{-1}$, $k_E^* = 10\,s^{-1}$, $k_1^* = 100\,\mu\text{M}^{-1}s^{-1}$ |
| Fig. 4D | $\rho_0$ = 0.02 $\mu$M, $[E_{ss}^*]$ = 0.01 $\mu$M, $k_1^* = 0.1\,\mu\text{M}^{-1}s^{-1}$, $V_c = 25000\,\mu\text{m}^3$ |
| Fig. 5B & D | $\rho_0$ = 0.5 $\mu$M, $[E]$ = 0.1 $\mu$M, $k^+ = 60\,\mu\text{M}^{-1}s^{-1}$, $k^* = 2000\,\mu\text{M}^{-1}s^{-1}$, $k_E^* = 10\,s^{-1}$, $k_1^* = 100\,\mu\text{M}^{-1}s^{-1}$ |
| Fig. 5C & E | $\rho_0$=0.033 $\mu$M, $k_0^+$= 60 $\mu\text{M}^{-1}\,s^{-1}$, $k_1^+$= 0.6 $\mu\text{M}^{-1}\,s^{-1}$ |
| Fig. 6B | $[\rho_a]$ = 0.25 $\mu$M, $[\rho_b]$ = 0.35 $\mu$M, $[\rho_E]$ = 0.015 $\mu$M, other parameters are same as below |
| Fig. 6C & D | $[\rho_a]$ = 0.25 $\mu$M, $[\rho_b]$ = 0.5 $\mu$M, $[\rho_E]$ = 0.01 $\mu$M, $k_a^+ = 10\,\mu\text{M}^{-1}s^{-1}$ $k_{b0}^+ = 0.5\,\mu\text{M}^{-1}s^{-1}$, $k_{b0}^- = 0.01\,s^{-1}$, |
| | $k_{aE}^+ = 5\times10^3\,\mu\text{M}^{-1}s^{-1}$, $k_{Eb}^+ = 10^3\,\mu\text{M}^{-1}s^{-1}$ $k_{b1}^+ = 10^4\,\mu\text{M}^{-1}s^{-1}$, $k_{b1}^- = 5\times10^{-3}\,s^{-1}$, $k_a^- = 5\times10^{-3}\,s^{-1}$ |
| Fixed parameters | $\delta v = 2\times10^{-4}\,\mu\text{m}^3$, $V_0 = 5\times10^{-3}\,\mu\text{m}^3$, $k^- = 5\times10^{-3}\text{s}^{-1}$, $V_c = 5000\,\mu m^3$ |

**Table 2.** Two component growth model across organisms

| | Component $a$ | Component $b$ | Enzyme $E$ | Reference |
|---|---|---|---|---|
| Fly | DSpd-2/Spd-2 | Cnn | Polo | (7, 12, 32) |
| Worm | SPD-2 | SPD-5 | PLK-1 | (29, 41) |
| Vertebrate | Cep192 | Cdk5Rap2/Cep215 | Plk1 | (42–44) |